Polymer Chemistry

Viscoelastic and Thermoreversible Networks Crosslinked by Non-covalent Interactions Between "Clickable" Nucleic Acids Oligomers and DNA

Journal:	*Polymer Chemistry*
Manuscript ID	PY-ART-01-2020-000165.R1
Article Type:	Paper
Date Submitted by the Author:	04-Mar-2020
Complete List of Authors:	Anderson, Alex; University of Colorado Boulder, Chemical and Biological Engineering Culver, Heidi; University of Colorado Boulder, Chemical and Biological Engineering Bryant, Stephanie; University of Colorado Boulder, Chemical and Biological Engineering Bowman, Christopher; University of Colorado Boulder, Chemical and Biological Engineering

Viscoelastic and Thermoreversible Networks Crosslinked by Non-covalent Interactions Between "Clickable" Nucleic Acids Oligomers and DNA

Alex J. Anderson[1], Heidi R. Culver[1], Stephanie J. Bryant[1,2,3], Christopher N. Bowman[1,2,3]

[1]Department of Chemical and Biological Engineering, University of Colorado, Boulder, CO 80303
[2]Material Science and Engineering Program, University of Colorado, Boulder, CO 80303
[3]BioFrontiers Institute, University of Colorado, Boulder, CO 80303

Abstract

An approach to efficient and scalable production of oligonucleotide-based gel networks is presented. Specifically, a new class of xenonucleic acid (XNA) synthesized through a scalable and efficient thiol-ene polymerization mechanism, "Clickable" Nucleic Acids (CNAs), were conjugated to a multifunctional poly(ethylene glycol), PEG. In the presence of complementary single stranded DNA (ssDNA), the macromolecular conjugate assembled into a crosslinked 3D gel capable of achieving storage moduli on the order of 1 kPa. Binding studies between the PEG-CNA macromolecule and complementary ssDNA indicate that crosslinking is due to the CNA/DNA interaction. Gel formation was specific to the base sequence and length of the ssDNA crosslinker. The gels were fully thermoreversible, completely melting at temperatures above 60°C and re-forming upon cooling over multiple cycles and with no apparent hysteresis. Shear stress relaxation experiments revealed that relaxation dynamics are dependent on crosslinker length, which is hypothesized to be an effect of the polydisperse CNA chains. Arrhenius analysis of characteristic relaxation times was only possible for shorter crosslinker lengths, and the activation energy for these gels was determined to be 110 ± 20 kJ/mol. Overall, the present work demonstrates that CNA is capable of participating in stimuli-responsive interactions that would be

expected from XNAs, and that these interactions support 3D gels that have potential uses in biological and materials science applications.

Introduction

Nucleic acids are powerful building blocks capable of directing the assembly of specific microstructures through Watson-Crick base pairing. Since the discovery of 2D and 3D DNA-directed nano-assembly of complex structures,[1,2] researchers have sought to design nucleic acid sequences and nucleic acid polymer conjugates for the development of functional materials. One primary advantage of structured DNA materials is their stimuli-responsiveness, or their ability to switch between two different states in response to an environmental change, which makes them ideal candidates for many biomedical applications such as biosensing and drug delivery.[3–6] For instance, Chaithongyot et al. applied DNA origami principles to design a cargo-loaded DNA nanosphere that opens in the presence of a cancer-specific protein marker.[5] Kahn and colleagues conjugated oligonucleotides to drug-loaded metal-organic frameworks and demonstrated pH and potassium ion triggered release.[6]

Recently, there has been a push to design macroscopic, 3D, DNA-based gels. These types of networks are crosslinked and solvent swollen materials that are also responsive to stimulus such as heat, pH, stress, or competitive binders. There are numerous examples in the literature of gels made from extracted DNA, which form hydrogels through physical entanglements,[7–9] or are chemically crosslinked by a bis-epoxide crosslinker.[8–11] With the development of automated DNA synthesis, examples of precisely structured DNA gels formed with rationally designed DNA oligonucleotides are expanding. These gels are typically designed to self-assemble into multifunctional building blocks with complementary “sticky-ends”, which hybridize to other building blocks to create an interconnected 3D network.[12–16] Yet another approach to creating stimuli-responsive DNA gels has been to conjugate oligonucleotides onto synthetic polymers and use them as crosslinkers.[17–27] These oligonucleotide-polymer hybrids offer many advantages such as diverse, multifunctional architectures, reduced cost due to shorter oligonucleotide requirements, and improved control over functionality and molecular weight.

While the potential applications of these materials have been demonstrated at a proof-of-concept level, the field has largely been held back by inherent drawbacks of oligonucleotide synthesis. Currently, the iterative, solid-phase approach is the prevailing synthetic scheme because of its ability to produce monodisperse DNA strands with precise sequence definition.[28,29] While the automation of this process has reduced the cost of oligonucleotide synthesis, the strategy still has characteristic disadvantages such as length restrictions and low yields, which severely limit large-scale implementation of DNA based technologies. Thus, there is a need for alternative synthetic approaches that are inexpensive, simple to execute, and have high yields while still affording the aforementioned advantages associated with DNA-based gels.

Click chemistries are ideally suited to address this issue, particularly when employed in a step-growth polymerization mechanism. To qualify as a click reaction, the transformation must reach quantitative conversions quickly and efficiently under ambient conditions with minimal byproducts. Some researchers have, for example, used a copper catalyzed, azide-alkyne cycloaddition to synthesize nucleic acid oligomers that bind to native DNA and are recognized by DNA polymerase.[30–32] However, this approach still requires a solid-phase support and iterative addition to reach lengths greater than 3 repeat units. Recently, a new generation of oligonucleotides, “Click” Nucleic Acids (CNAs), have been developed to circumvent these synthesis inefficiencies while maintaining the capacity to hybridize with complementary nucleic acid sequences.[33,34] CNAs fall into a class of molecules known as xenonucleic acids (XNAs), or nucleic acids with non-natural backbones.[35,36] Specifically, CNAs are synthesized through a radical mediated, linear thiol-ene “click” polymerization mechanism. Previous work has shown that CNAs are readily conjugated to synthetic polymers through thiol-ene or thiol-Michael mechanisms, are capable of binding to complementary ssDNA strands, and are cytocompatible,[37,38] making them promising candidates for nucleic acid-based biomaterials.

Herein, the development of a 3D gel reversibly crosslinked by sequence specific interactions between CNA and a complementary DNA strand is reported. These CNA/DNA gels are shown to exhibit complex viscoelastic responses to mechanical stimuli, as well as rapid and complete thermoreversibility.

This work establishes CNA/DNA gels as a material capable of stimuli-responsive behavior with potential use in a variety of biological and materials science applications.

Materials and Methods

Synthesis of 8PEG-T macromolecule

Thymine CNA monomer was synthesized as described previously with a slight adjustment.[34] Here, the thymine nucleobase was protected with a tert-butoxycarbonyl (BOC) group at the imide prior to backbone addition. The thiol functionality on the monomer was deprotected by dissolving the monomer in methanol (0.5 M) and at least two equivalents of sodium hydroxide (NaOH) for 5-10 minutes. The reaction was neutralized with excess phosphate buffered saline (PBS) and an equimolar amount of hydrochloric acid (HCl). The monomer was extracted into dichloromethane (DCM) and dried over sodium sulfate. The solvent was removed by vacuum yielding dry, deprotected CNA monomer. This monomer was combined with 8-arm poly(ethylene glycol) thiol (20,000 g/mol, Jenkem USA) at a 15:1 monomer to arm ratio, and dissolved at 17% weight (with respect to monomer) in dimethyl sulfoxide (DMSO) containing 0.1% weight DMPA as a photoinitiator and 2.5% weight tris(2-carboxyethyl)phosphine HCl (TCEP HCl). The TCEP HCl was included to protect against the formation of disulfides during the polymerization. The mixture was polymerized with 365 nm UV light at 12 mW/cm^2 for 15 minutes. The crude product mixture was directly dialyzed against DMSO (20,000 MWCO) to remove unbound and/or unreacted CNA. The dry, solid product was obtained after lyophilization of the DMSO solvent. Gel permeation chromatography (GPC) was used to qualitatively confirm the molecular weight increase of the copolymer and ^1H NMR was used to quantify the number average degree of polymerization per PEG arm. The number average degree of polymerization was used to approximate the molecular weight of the 8PEG-T macromer. Prior to gel formation, the solid product was dissolved in a 1:2 ratio of DCM to trifluoroacetic acid (TFA) to remove the BOC protecting group and subsequently precipitated in ether. The product was washed extensively with ether to remove all TFA.

Microscale Thermophoresis (MST) Titration

8PEG-T was dissolved at 31.2 mM in DMSO to achieve a 250 uM CNA oligomer end group concentration. This stock was then serially diluted 1:2 to create a ligand titration curve. A DNA "pre-mix" solution was prepared by mixing 150 μL DMSO, 50 μL MilliQ H_2O, 25 μL 0.66X saline sodium citrate (SSC) buffer, and 25 μL of 1 μM A20-Cy5 DNA in 0.66X SSC buffer. Equal volumes of each 8PEG-T stock and the "pre-mix" solution were mixed and vortexed, for a final DMSO concentration of 80 vol%, CNA concentration of 125 μM, and DNA concentration of 50 nM. Each sample was centrifuged to remove insoluble fractions and 13 μL were taken to load into MST capillaries. MST traces were measured on a Nanotemper Monolith NT.115 at a temperature of 23°C using the red LED operating at 14% power and the 1475 nm infrared (IR) laser operating at 80% power. The ratio of the average fluorescence before (-1 – 0s, F_{cold}) and after (0.5 – 1.5 s, F_{hot}) turning on the IR laser (at 0 s) was taken as the normalized fluorescence (i.e., $F_{norm} = F_{cold}/F_{hot}$). F_{norm} was plotted against the $\log_{10}$ of CNA concentration and fit to the Hill Model to obtain an apparent dissociation constant (K_d').

Circular Dichroism

For circular dichroism experiments, the copolymer was dissolved at 50 μM in 20% H_2O in DMSO containing 25 μM A20 ssDNA. These concentrations were chosen to ensure no gel formed in the cuvette. CD spectra were obtained on an Applied Photophysics Chirascan Plus CD spectrometer in a quartz cuvette with a 0.5 mm pathlength, using a 1 nm step size and a 1 nm bandwidth, with a time per point of 0.5 seconds. To determine CNA/DNA melting, the temperature was varied from 12.5°C to 50°C at a rate of 2°C/min using a Peltier controlled sample holder, and the temperature inside the cuvette was monitored using in-cell temperature sensors.

Gel Formation

All gels were made at a 5% w/v 8PEG-T concentration in 80% DMSO/20% DI H_2O. The amount of ssDNA added was calculated by the required CNA:DNA base ratio. Gels were formed by separately dissolving 8PEG-T and ssDNA in solvent to confirm that the individual components alone did not form a gel upon macroscopic visualization. After mixing the two components, the solution was set at room

temperature. Gel formation was verified by assessing its stability upon inversion and mechanical agitation.

Rheological Characterization

Oscillatory shear rheology was carried out on gels with an Ares G2 Rheometer (TA Instruments). In a typical experiment, the gel was heated above its reverse gelation temperature and an aliquot was placed between a parallel plate geometry. The bottom plate consisted of the Advanced Peltier Systems (TA Instruments) geometry, and the thermally insulating top plate was 8 mm in diameter. The evolution of modulus was monitored at 0.5% strain and 1 Hz. The thermal sensitivity of CNA gels was characterized at 5% strain and 1 Hz while cycling the temperature between 70°C and 22°C at 5°C/min. Strain sweeps were conducted at 1.6 Hz and frequency sweeps at 5% strain. Stress relaxation was performed with a 10% initial strain applied immediately. To prevent solvent evaporation during experiments, a thin layer of light mineral oil was added around the sample.

Statistical Analysis

Unless otherwise stated, data are presented are representative of multiple replicates. Statistical significance was defined at the 95% confidence level ($p<0.05$) using appropriate ANOVA analysis. In cases where significance was detected, Tukey's Post Hoc analysis was used for pair-wise comparisons.

Results and Discussion

Synthesis of 8PEG-T macromolecule

The CNA polymerization follows a thiol-ene click mechanism that results in linear oligomers of nucleic acids (Figure 1a). To create a multifunctional macromolecule, a thiolated 8-armed poly(ethylene glycol) (8PEG-SH) star polymer was doped into the CNA polymerization at a 15:1 thymine monomer to PEG arm ratio. The mixture was combined with a photoinitiator (0.1% DMPA) and TCEP HCl (a reducing agent to prevent disulfide formation) and irradiated with UV light. The terminal thiols of the 8PEG-SH served as conjugation points for the CNA, resulting in a star block-copolymer with pendant CNA oligomers. Linear thiol-ene polymerization has been shown to yield polymers and oligomers quickly and efficiently,[39,40] but it is important to note that the thiol-ene polymerization mechanism for this

particular reaction is quasi step-growth and results in a polydisperse product. Therefore, there is a distribution of CNA monomers per arm, ranging, for example, from monomers or dimers to 20+-mers. For situations in which polydispersity can be tolerated, this synthetic scheme provides a clear advantage in simplicity and efficiency over other polymerizations strategies. After polymerization, the majority of unreacted CNA monomer and shorter oligomers were removed by dialysis, and the CNA was deprotected with acid. After extensive washing, the resulting product was analyzed with GPC and ^{1}H NMR (Supporting Figures S1 and S2). Relative integration of protons indicated the achieved degree of polymerization was between 10 and 12 repeat units, depending on the batch, which effectively doubles the molecular weight of each arm (i.e. 2500 g/mol PEG and 2700 g/mol CNA). This scheme yields a co-polymer product with average molecular weights around 42,000 g/mol. The molecular weight increase in GPC traces qualitatively supported this finding. ^{1}H NMR also showed complete deprotection of the BOC group.

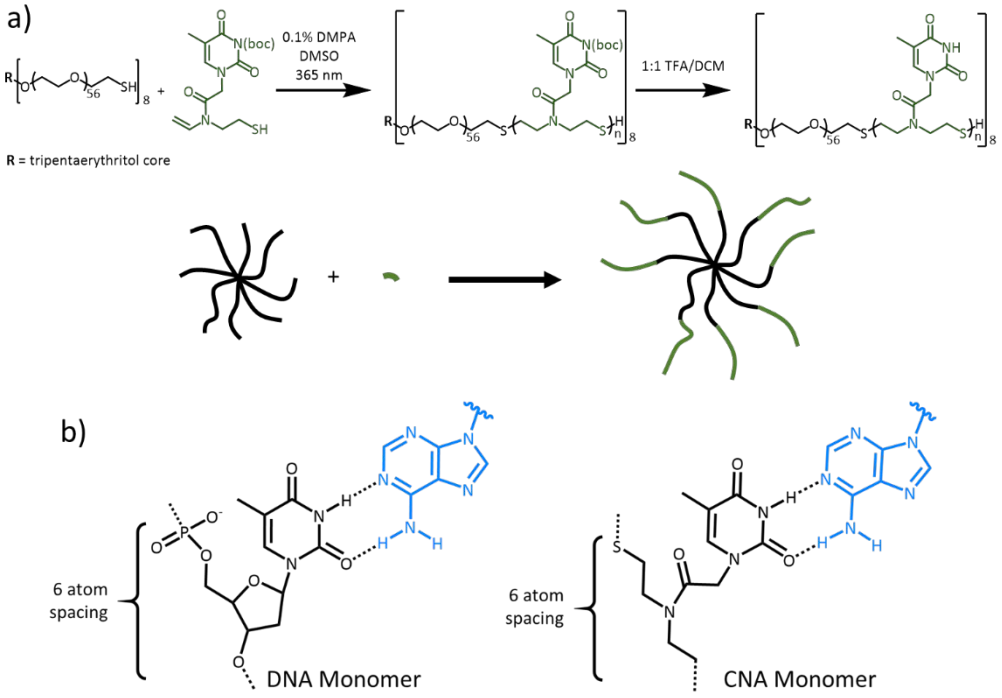

Figure 1 - a) Synthesis of 8PEG-T was achieved through a copolymerization technique. The solid product was obtained after dialysis and deprotection. b) Comparison between a DNA monomer and CNA monomer. The CNA repeat unit maintains the 6-atom spacing allowing for the hybridization to complementary nucleic acids.

CNA monomers were specifically designed to bind to DNA.[33,34] A comparison of a thymine CNA repeat unit and a thymine DNA repeat unit binding to a complementary nucleotide is shown in Figure 1b. The differences between the two monomers are primarily in the backbone, where the CNA monomer avoids the deoxyribose sugar and phosphate group and is instead linked by a thioether bond. However, the conserved 6-atom spacing between repeat units allows for efficient hydrogen bonding between complementary nucleotides.

Binding of 8PEG-T to Polyadenine DNA

The binding of thymine CNA oligomers and complementary adenine ssDNA has been investigated previously, and it has been shown that binding is achieved in solution at relatively low concentrations.[34] MST and CD spectroscopy were employed to confirm that binding was not affected by the conjugation of the thymine oligomers to a PEG macromolecule. A typical MST titration experiment is used to evaluate the binding of a ligand to a fluorescent analyte by tracking the change in the rate of diffusion of the unbound analyte and the bound analyte in a microscale temperature gradient.[41] By titrating in the ligand, the multiarmed 8PEG-T, while keeping the fluorescent analyte concentration constant, A20-Cy5 DNA at 50 nM, a binding curve was created and the apparent dissociation constant (K_d') extrapolated.

Figure 2a shows an MST titration for the 8PEG-T macromolecule and a fluorescent A20 analyte in 80% DMSO/20% H_2O (v/v). This solvent mixture was chosen for two reasons. Primarily, the 8PEG-T macromolecule is not water-soluble and requires the presence of a significant amount of DMSO to dissolve; at higher DMSO concentrations 90% and above, however, 8PEG has limited solubility. Additionally, on-going studies have shown that CNA-DNA exhibits weak hybridization beyond 80% DMSO. The sigmoidal increase in normalized fluorescence indicates a significant binding event that corresponds to an apparent dissociation constant (K_d') of 19.5 μM. The K_d' of unconjugated, homothymine CNA polymers was previously found to be 70 μM in 50/50 aqueous/DMSO mixture.[34] The difference between the experimental conditions is likely the primary reason for the decrease in K_d' as the 80/20 system has been found to be better for CNA/DNA binding than the 50/50 system (unpublished

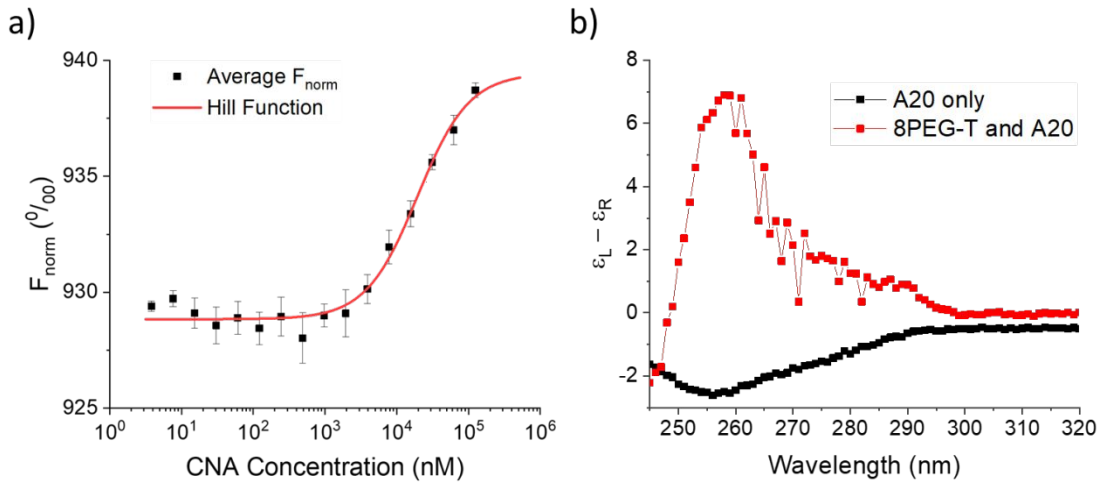

Figure 2. a) Microscale thermophoresis titration experiment showing binding between 8PEG-T and a Cy-5 labelled A20 ssDNA. Solvent was 20% H_2O in DMSO. A20 DNA was supplied at 50 nM. Data points are averages of technical replicates, n=3. b) Circular dichroism of A20 ssDNA only and A20 bound to 8PEG-T. The profile of the 8PEG-T alone was subtracted out of the spectra showing binding (red curve). Spectra are averages of technical replicates, n=3.

observations). However, the result confirms that PEGylation of the CNA oligomer does not interfere with ssDNA binding.

Circular dichroism was then used to study the binding event directly and the effect it has on ssDNA conformation. Figure 2b shows the CD spectra of A20 DNA before and after the addition of the 8PEG-T macromolecule. In pure aqueous environments, the CD spectrum of single stranded poly(A) DNA exhibits a positive Cotton effect with zero crossing at 260 nm, which is attributed to base stacking.[42] However, in a 20% H_2O/80% DMSO, A20 ssDNA exhibits a shallow, negative peak around 250-260 nm, suggesting limited base stacking in this solvent system. Upon introduction of the complementary 8PEG-T macromolecule, the structure clearly changes, as evidenced by the inversion of the peak at 260 nm. This spectrum is similar to duplexes in solutions with a high ethanol fraction. This behavior suggests that the duplex adopts a dehydrated A-form, as evidenced by the maximum around 260 nm with a shoulder that persists to around 290 nm.[42] However, additional studies must be performed to describe fully the molecular structure of the CNA/DNA interaction in this solvent system.

Formation of CNA/DNA gels

Gels were created using the 8PEG-T macromolecule by mixing with different types and lengths of ssDNA. 8PEG-T and ssDNA crosslinker were separately dissolved in 20% H_2O in DMSO at the same concentrations to confirm that each component alone did not result in a gel. It is important to note here that the synthetic scheme leaves each 8PEG-T arm with a thiol end group that could potentially form disulfide bonds. However, the observation that 8PEG-T does not form gels on its own suggests that disulfides do not significantly contribute to crosslinking. Because each arm of 8PEG-T has on average 10-12 thymine repeat units, it was hypothesized that a 40-mer homopolymer of adenine ssDNA (A40) would be sufficient to connect adjacent 8PEG-T macromers. The two components were then simply mixed, vortexed, and allowed to set at room temperature. The final gel formulation consisted of 5% w/v 8PEG-T and a 1:1 adenine:thymine ratio (e.g. a 4:1 CNA oligomer to A40 ratio). At this ratio, each CNA base has the potential to interact with a DNA base to ensure the amount of DNA added is sufficient to crosslink the network. Attempts to de-gel the sample by strand exchange with T40 ssDNA were unsuccessful due to

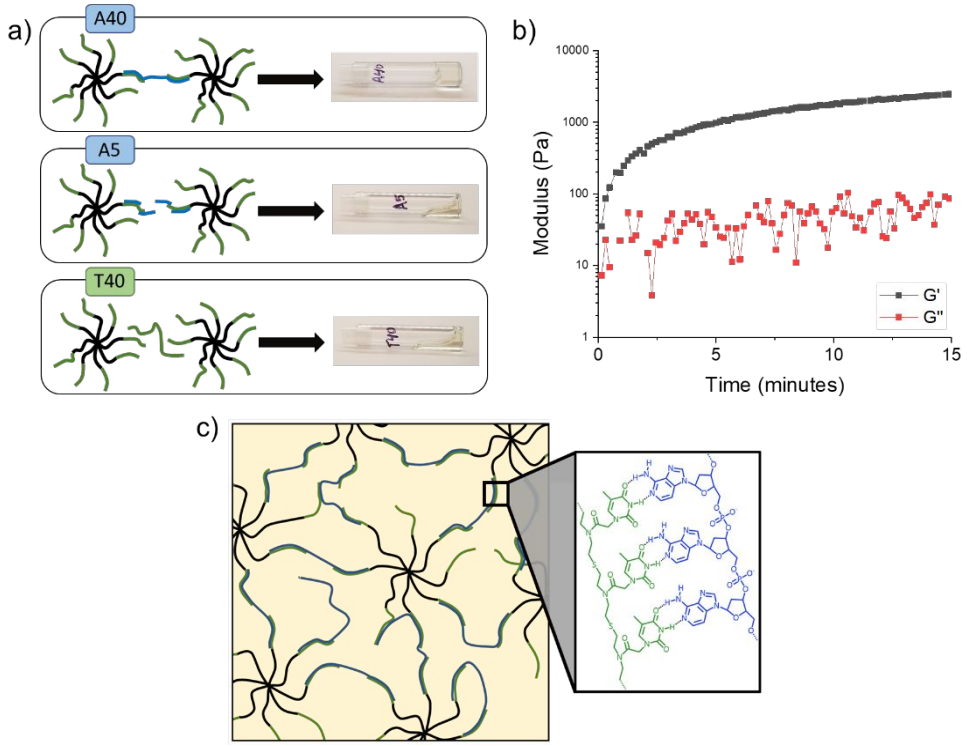

Figure 3. a) Gels only form when the ssDNA crosslinker is complementary and sufficiently long enough to bridge two adjacent 8PEG-T molecules b) The CNA/DNA gel's modulus was tracked as a function of time, rising to over 1 kPa in around 10 min. Rheology done at 0.1% strain and 1 Hz. c) Hypothesized mechanism of gelation including cycles and the potential for multiple CNA oligomers to bind to one ssDNA crosslinker

complete destabilization of DNA/DNA duplexes in solutions with greater than 60% DMSO content.[43] Gel formation was tracked by oscillatory shear rheology and began as soon as the experiment was initiated (Figure 3b). The storage modulus of this gel formulation evolved quickly, reaching a plateau in the range of 500-1000 Pa in about 15 minutes.

To test the sensitivity of the gel to the type of ssDNA crosslinker, a 40-mer homopolymer of thymine (T40) and a 5-mer homopolymer of adenine (A5) were used. The T40 ssDNA does not interact specifically with the thymine CNA and was used to assess CNA/DNA binding specificity.[34] The A5 ssDNA is too short to bridge two adjacent CNA arms and was used to assess the role of crosslinker length. In each case 8PEG-T was held at 5% w/v and a 1:1 CNA base to DNA base ratio was used. Neither crosslinker led to gelation, which was confirmed by the flow observed upon vial inversion. These findings, when coupled with data from binding studies, indicate that gelation is due to sequence specific base-pairing between the thymine CNA chains and the complementary DNA crosslinker. A general structure of the gel and how it is crosslinked with DNA is proposed in Figure 3c, which shows possible effective crosslinks, the potential for dangling chains and cycles, and the possibility of more than two CNA oligomers to interact with one A40 strand.

CNA/DNA gels are thermoreversible

Because CNA/DNA gels are crosslinked by temperature sensitive hydrogen bonding, the gel mechanics should be sensitive to stimuli that disrupt these interactions. For instance, high temperatures lead to the dissociation of double stranded nucleic acids, and it would therefore be expected that gels made based on these interactions would undergo a gel-sol transition at elevated temperatures. This phenomenon is well documented for DNA/DNA gels and similar materials.[10,13,44,45] Shear rheology was used to track the modulus as a function of temperature to study the thermosensitivity of CNA/DNA gels. Upon increasing the temperature from 22°C to 70°C, the gels change from a predominantly elastic solid to an unstructured liquid (Figure 4a). Cooling the liquid back to room temperature caused the gel to regain its structure and evolve to a modulus of the same order of magnitude as the initial gel. Importantly, the gel fully “melts” and reforms with repeated heat/cool cycles, indicating complete thermoreversibility through

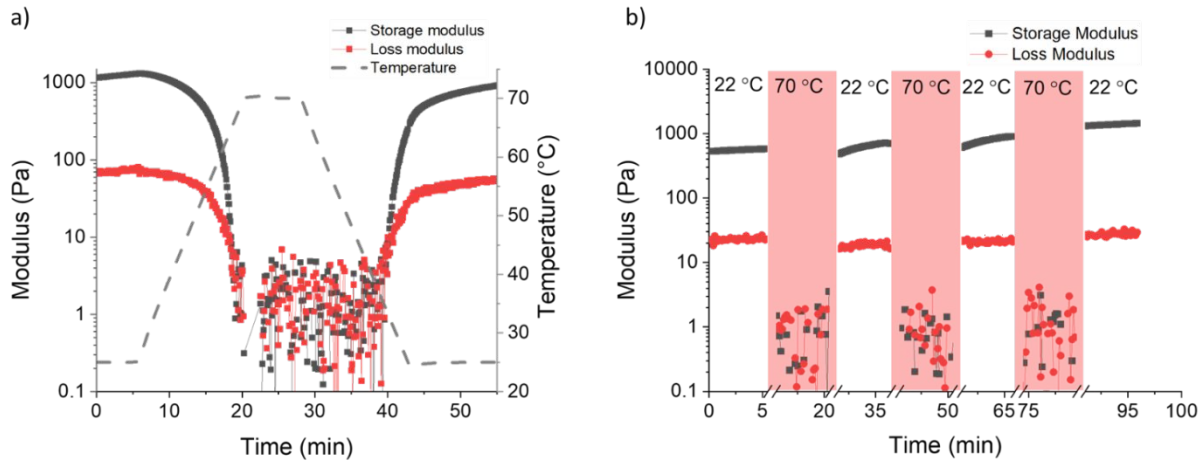

Figure 4 – a) Melting and reconstitution of the CNA/DNA gel. Gels were made at 5% w/v 8PEG-T, with an A40 ssDNA, at 1:1 A:T, in 20% H_2O in DMSO. Rheology was performed at 5% strain at 1 Hz. b) Thermal cycles of CNA/DNA gels showing complete reversibility.

at least the three cycles assessed here (Figure 4b). One interesting observation of this thermoreversibility is that the gel stiffness appears to increase with each successive cycle (Supporting Figure S3). This observation could be explained by artifactual effects such as unavoidable solvent loss during the heating process, or by material specific phenomena such as increased crosslinking with successive cycles. The latter effect has been observed previously in DNA gels and has been hypothesized to be a result of the reorganization of the nucleic acid strands upon dissociation, leading to more crosslinks and entanglements upon reassociation.[8,10]

To understand further the gel-to-sol transition, the CD spectrum was measured as a function of temperature to investigate the CNA/DNA melting process (Figure 5a). The change in CD at 290 nm indicates that the melting temperature is 24.5°C in 80% DMSO/20% H_2O. This temperature is comparable to the melting temperature of an A12/T12 DNA duplex (aqueous, 0.05 M NaCl) at a similar concentration.[46,47] The melting curve obtained from CD measurements can be interpreted as a representation of the percent of intact CNA/DNA interactions as a function of temperature. Therefore, based on this curve, all duplexes would be expected to be dissociated at temperatures of 40°C and higher. In the context of the CNA/DNA gel, this would lead to complete reverse gelation. Experimentally, however, the gels tolerated higher temperatures, ultimately "melting" above 60°C during rheological temperature sweeps (e.g. Figure 4a). To confirm this observation was not due to slow kinetics of de-

gelation, a second temperature sweep was performed with 60°C as the maximum instead of 70°C (Supporting Figure S4). The gel maintained its elasticity at 60°C, confirming that a higher temperature is needed for reverse gelation to occur.

One possible explanation for this phenomenon is the concentration dependence of nucleic acid

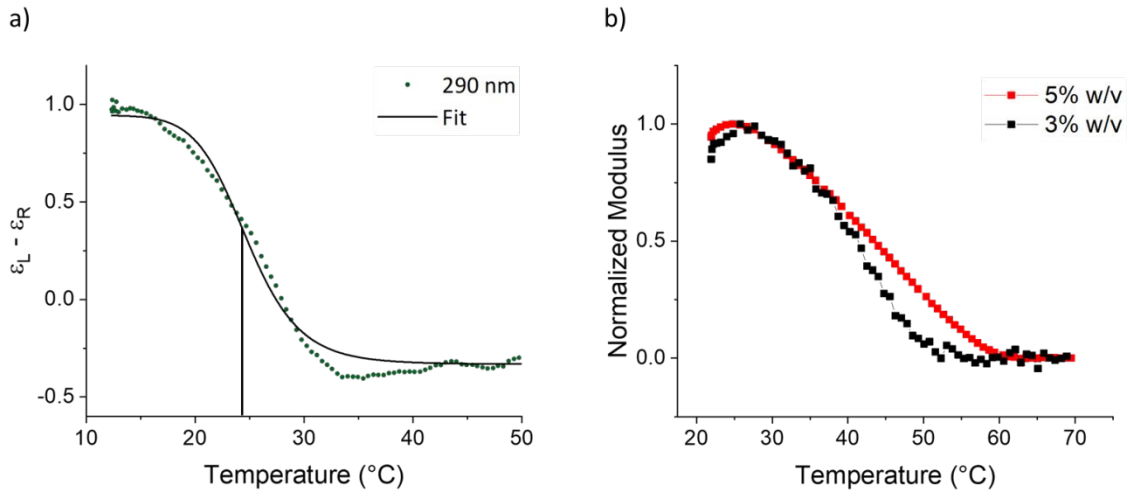

Figure 5 – a) Circular dichroism of the melting transition of 8PEG-T and A20. The signal at 290 nm was tracked as a function of temperature and fit to a sigmoidal decay curve yielding a melting point of 24.5°C. Data points are averages of technical replicates, n=3. b) CNA/DNA gels were prepared at either 5% w/v or 3% w/v 8PEG-T and subjected to thermally induced melting. The gels were found to melt quicker and at a lower temperature at 3% w/v than at 5% w/v.

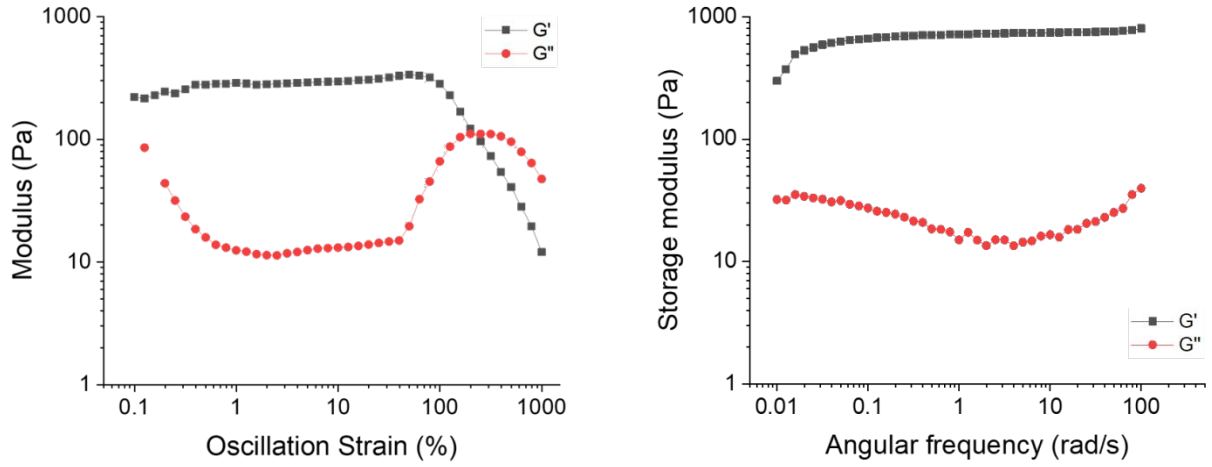

Figure 6 – (a) Oscillation sweep of 5% w/v CNA/DNA gel. (b) Frequency sweep of 5% w/v CNA/DNA gel. Gels were made with a 1:1 A:T ratio, in 20% H_2O in DMSO. Plots are representative of 3 replicates.

melting temperatures.[7,48] In this study, the dilute concentration at which the melting temperature was measured (0.3% w/v) by CD and the concentration used to form a gel (5% w/v) differed by an order of magnitude, potentially explaining the large discrepancy. To investigate whether this dependence is present in the CNA/DNA system, gels were made at 3% w/v 8PEG-T and the same 1:1 A:T ratio and the shear modulus was tracked as a function of temperature. The temperature at which reverse gelation was achieved for the 3% w/v gel was 52 ± 5°C, which was significantly lower than 61 ± 3°C, the temperature at which the 5% w/v gel reached reverse gelation. To ensure this behavior was not due to differences in gel stiffness, the normalized modulus was plotted as a function of temperature to compare the "melting" rate of each gel (Figure 5b). The less concentrated gel "melted" faster and at lower temperatures than the more concentrated gel. These results confirm that concentration plays a significant role in the temperature dependence of CNA/DNA gels. However, other interactions may be contributing to this discrepancy, such as phase separation between the hydrophilic PEG block and the relatively hydrophobic CNA block. These and other physical interactions could lead to additional non-covalent interactions with different temperature dependencies and result in the increased reverse gelation temperature.

Understanding the CNA/DNA interaction within the gel network

To understand further the CNA/DNA interactions and how they contribute to the mechanical properties of the gel, the viscoelastic response to various mechanical stimuli was investigated using shear rheology. First, strain amplitude sweeps were conducted on A40 crosslinked gels (5% w/v, 1:1 A:T) to identify the linear viscoelastic region (LVR). The LVR persisted to about 45% strain and the elasticity was maintained to about 200% strain, which is the point at which all crosslinks were disrupted and the gel began to flow (Figure 6a). With knowledge of the LVR, frequency sweeps were performed to identify the viscoelastic response of the gel to an oscillating strain. Based on Semenov and Rubenstein's theory of reversible networks, the material's frequency response can be used to extract information about the lifetimes of the reversible interactions. Specifically, the crossover between storage modulus (G') and loss modulus (G") provides a good estimation of the lifetime of the crosslinking interaction. In the range examined, CNA/DNA gels exhibited clear frequency dependent behavior, primarily evident by the U-shaped loss modulus curve. Furthermore, G' and G" crossover was not captured in the experiment, but appears to occur at frequencies below 0.01 rad/s, indicating a long lifetime of the reversible crosslink (Figure 6b), consistent with studies performed with DNA crosslinked polyacrylamide hydrogels.[25]

Stress relaxation experiments were performed on A40 crosslinked gels (5% w/v, 1:1 A:T) and at different temperatures. These experiments were used to determine the kinetic dissociation rate constant, which is correlated to the lifetime of the crosslinking interaction.[49,50] Further, by plotting either the relaxation rates or characteristic relaxation times as a function of temperature in an Arrhenius plot, the activation energy required for the crosslink breakage was also determined. Stress relaxation plots were fit with a form of the Kohlrausch-Williams-Watts stretched exponential function, which has been shown to adequately describe viscoelastic systems.[51–53] Surprisingly, the relaxation profiles did not change as a function of temperature from 15 °C to as high as 50 °C, nearing the reverse gelation temperature (Figure 7a). The calculated relaxation time constants also showed no difference with temperature.

One hypothesis for this behavior is related to the 8PEG-T structure. The CNA polymerization is a step-growth mechanism resulting in polydisperse CNA chains. This polydispersity will yield a spectrum

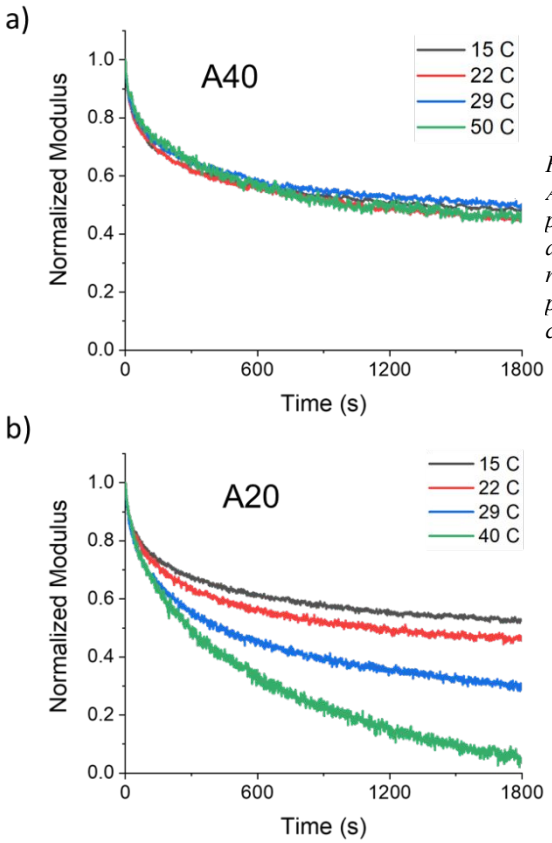

Figure 7 – Representative stress relaxation plots for (a) A40 crosslinker and (b) A20 crosslinker. Relaxation profiles overlap regardless of the temperature with A40 as the crosslinker, but exhibit temperature dependent relaxation with the A20 crosslinker. Rheology was performed with a 10% immediate initial strain in both cases.

of crosslinking interactions with different numbers of base pairs. This crosslinking landscape would result in a spectrum of binding energies and melting temperatures. Thus, as temperature is increased, low energy, short CNA/DNA interactions with relatively few base pairs will break, while long CNA/DNA interactions, which have higher energy from additional base pairing, will persist. As a result, the average number of base pairs contributing to a crosslink (as well as the thermodynamic stability of the crosslink) will increase with increasing temperature. Thus, the relaxation profiles in Figure 7a may be dominated by the long CNA/DNA chain interactions. It stands to reason if the longer crosslinking interactions with more base pairs are eliminated, the temperature independence due to differences in the crosslink lengths could be mitigated and an Arrhenius dependence would be observed. Indeed, when the DNA crosslinker was shortened to A20 while maintaining a 5% w/v 8PEG-T concentration and a 1:1 A:T ratio, temperature dependent stress relaxation was observed (Figure 7b). It should be noted that for both the

A40 and A20 crosslinkers, the stress relaxation profiles at the lower temperatures appear similar, relaxing about 50% of their original stress within 30 minutes. These profiles were fit to the KWW model and the characteristic relaxation time constants were calculated. The Arrhenius activation energy for crosslink relaxation in this system was determined to be 110 ± 20 kJ/mol (Supporting Figure S5). As a comparison, the activation energy for dsDNA of a comparable length (in aqueous conditions, ~1M NaCl) has been found to be approximately 220 kJ/mol.[54,55]

Conclusion

In this work the ability of CNAs to participate in reversible interactions with complementary ssDNA was exploited to develop stimuli-responsive, 3D gels. Single molecule binding experiments confirmed the interaction between the CNA functionalized multi-arm macromolecule, 8PEG-T, and a complementary adenine ssDNA. When 8PEG-T and a complementary ssDNA crosslinker were mixed in a more concentrated solution, gels formed and reached a modulus on the order of 1 kPa. Furthermore, these gels were viscoelastic, thermoreversible, and stress relaxing, which is consistent for physically crosslinked materials. Several features of the responsive behavior of the gel highlight unique attributes of the CNA/DNA system, which include a strong concentration dependent “melting” and complex hybridization dynamics due to the polydispersity of the CNA oligomers. This work demonstrates the ability for CNA to facilitate stimuli responsive crosslinking and create reversible 3D gel materials for future biological and materials science applications.

Conflicts of interest

The authors do not declare any conflicts of interest

Acknowledgments.

The authors would like to acknowledge Mingtao Chen, Jasmine Singha, and Benjamin Fairbanks for helpful discussion and input in the preparation of this manuscript. This work was completed with support from an NSF MRSEC grant (DMR 1420736) and from a US Department of Education GAANN Fellowship to Alex Anderson.

References

1 N. C. Seeman, *J. Theor. Biol.*, 1982, **99**, 237–247.
2 J. Chen and N. C. Seeman, *Nature*, 1991, **350**, 631–633.
3 C. Wang, J. Ren and X. Qu, *Chem. Commun.*, 2011, **47**, 1428–1430.
4 T. Goda and Y. Miyahara, *Biosens. Bioelectron.*, 2012, **32**, 244–249.
5 S. Chaithongyot, N. Chomanee, K. Charngkaew, A. Udomprasert and T. Kangsamaksin, *Mater. Lett.*, 2018, **214**, 72–75.
6 J. S. Kahn, L. Freage, N. Enkin, M. A. A. Garcia and I. Willner, *Adv. Mater.*, 2017, **29**, 1602782.
7 N. Arfin, V. K. Aswal, J. Kohlbrecher and H. B. Bohidar, *Polymer*, 2015, **65**, 175–182.
8 O. Okay, *J. Polym. Sci. Part B Polym. Phys.*, 2011, **49**, 551–556.
9 P. Karacan, H. Cakmak and O. Okay, *J. Appl. Polym. Sci.*, 2013, **128**, 3330–3337.
10 F. Topuz and O. Okay, *Macromolecules*, 2008, **41**, 8847–8854.
11 F. Topuz, S. Singh, K. Albrecht, M. Möller and J. Groll, *Angew. Chem. Int. Ed.*, 2016, **55**, 12210–12213.
12 R. Cao, Z. Gu, L. Hsu, G. D. Patterson and B. A. Armitage, *J. Am. Chem. Soc.*, 2003, **125**, 10250–10256.
13 Y. Xing, E. Cheng, Y. Yang, P. Chen, T. Zhang, Y. Sun, Z. Yang and D. Liu, *Adv. Mater.*, 2011, **23**, 1117–1121.
14 J. Fernandez-Castanon, S. Bianchi, F. Saglimbeni, R. D. Leonardo and F. Sciortino, *Soft Matter*, 2018, **14**, 6431–6438.
15 S. H. Um, J. B. Lee, N. Park, S. Y. Kwon, C. C. Umbach and D. Luo, *Nat. Mater.*, 2006, **5**, 797–801.
16 M. Nishikawa, Y. Mizuno, K. Mohri, N. Matsuoka, S. Rattanakiat, Y. Takahashi, H. Funabashi, D. Luo and Y. Takakura, *Biomaterials*, 2011, **32**, 488–494.
17 T. Liedl, H. Dietz, B. Yurke and F. Simmel, *Small*, 2007, **3**, 1688–1693.
18 B. Wei, I. Cheng, K. Q. Luo and Y. Mi, *Angew. Chem. Int. Ed.*, 2008, **47**, 331–333.
19 Y. Hu, W. Guo, J. S. Kahn, M. A. Aleman-Garcia and I. Willner, *Angew. Chem. Int. Ed.*, 2016, **55**, 4210–4214.
20 Y. Murakami and M. Maeda, *Macromolecules*, 2005, **38**, 1535–1537.
21 L. Peng, M. You, Q. Yuan, C. Wu, D. Han, Y. Chen, Z. Zhong, J. Xue and W. Tan, *J. Am. Chem. Soc.*, 2012, **134**, 12302–12307.
22 B. Yurke, *J. Biomech. Eng.*, 2004, **126**, 104.
23 F. X. Jiang, B. Yurke, B. L. Firestein and N. A. Langrana, *Ann. Biomed. Eng.*, 2008, **36**, 1565–1579.
24 F. X. Jiang, B. Yurke, R. S. Schloss, B. L. Firestein and N. A. Langrana, *Biomaterials*, 2010, **31**, 1199–1212.
25 C. Du and R. J. Hill, *Macromolecules*, 2019, **52**, 6683–6697.
26 S. Tanaka, S. Yukami, K. Fukushima, K. Wakabayashi, Y. Ohya and A. Kuzuya, *ACS Macro Lett.*, 2018, **7**, 295–299.
27 S. Tanaka, K. Wakabayashi, K. Fukushima, S. Yukami, R. Maezawa, Y. Takeda, K. Tatsumi, Y. Ohya and A. Kuzuya, *Chem. – Asian J.*, 2017, **12**, 2388–2392.
28 M. D. Matteucci and M. H. Caruthers, *J. Am. Chem. Soc.*, 1981, **103**, 3185–3191.
29 S. L. Beaucage and M. H. Caruthers, *Tetrahedron Lett.*, 1981, **22**, 1859–1862.
30 H. Isobe, T. Fujino, N. Yamazaki, M. Guillot-Nieckowski and E. Nakamura, *Org. Lett.*, 2008, **10**, 3729–3732.
31 A. H. El-Sagheer and T. Brown, *Chem. Commun.*, 2011, **47**, 12057–12058.

32 A. H. El-Sagheer, A. P. Sanzone, R. Gao, A. Tavassoli and T. Brown, *Proc. Natl. Acad. Sci.*, 2011, **108**, 11338–11343.
33 W. Xi, S. Pattanayak, C. Wang, B. Fairbanks, T. Gong, J. Wagner, C. J. Kloxin and C. N. Bowman, *Angew. Chem. Int. Ed.*, 2015, **54**, 14462–14467.
34 X. Han, D. W. Domaille, B. D. Fairbanks, L. He, H. R. Culver, X. Zhang, J. N. Cha and C. N. Bowman, *Biomacromolecules*, 2018, **19**, 4139–4146.
35 B. D. Fairbanks, H. R. Culver, S. Mavila and C. N. Bowman, *Trends Chem.*, , DOI:10.1016/j.trechm.2019.06.004.
36 K. Morihiro, Y. Kasahara and S. Obika, *Mol. Biosyst.*, 2017, **13**, 235–245.
37 A. J. Anderson, E. B. Peters, A. Neumann, J. Wagner, B. Fairbanks, S. J. Bryant and C. N. Bowman, *Biomacromolecules*, 2018, **19**, 2535–2541.
38 Harguindey Albert, Domaille Dylan W., Fairbanks Benjamin D., Wagner Justine, Bowman Christopher N. and Cha Jennifer N., *Adv. Mater.*, 2017, **29**, 1700743.
39 V. S. Khire, T. Y. Lee and C. N. Bowman, *Macromolecules*, 2008, **41**, 7440–7447.
40 J. M. Sarapas and G. N. Tew, *Macromolecules*, 2016, **49**, 1154–1162.
41 M. Jerabek-Willemsen, T. André, R. Wanner, H. M. Roth, S. Duhr, P. Baaske and D. Breitsprecher, *J. Mol. Struct.*, 2014, **1077**, 101–113.
42 D. M. Gray, R. L. Ratliff and M. R. Vaughan, in *Methods in Enzymology*, Academic Press, 1992, vol. 211, pp. 389–406.
43 X. Wang, H. J. Lim and A. Son, *Environ. Health Toxicol.*, , DOI:10.5620/eht.2014.29.e2014007.
44 S. Nagahara and T. Matsuda, *Polym. Gels Netw.*, 1996, **4**, 111–127.
45 H. Kang, A. C. Trondoli, G. Zhu, Y. Chen, Y.-J. Chang, H. Liu, Y.-F. Huang, X. Zhang and W. Tan, *ACS Nano*, 2011, **5**, 5094–5099.
46 J. SantaLucia and D. Hicks, *Annu. Rev. Biophys. Biomol. Struct.*, 2004, **33**, 415–440.
47 S. M. Freier, R. Kierzek, J. A. Jaeger, N. Sugimoto, M. H. Caruthers, T. Neilson and D. H. Turner, *Proc. Natl. Acad. Sci. U. S. A.*, 1986, **83**, 9373–9377.
48 T. G. Mason, A. Dhople and D. Wirtz, *Macromolecules*, 1998, **31**, 3600–3603.
49 G. A. Parada and X. Zhao, *Soft Matter*, , DOI:10.1039/C8SM00646F.
50 M. Rubinstein and A. N. Semenov, *Macromolecules*, 1998, **31**, 1386–1397.
51 N. Sasaki, Y. Nakayama, M. Yoshikawa and A. Enyo, *J. Biomech.*, 1993, **26**, 1369–1376.
52 A. Hotta, S. M. Clarke and E. M. Terentjev, *Macromolecules*, 2002, **35**, 271–277.
53 F. Meng, R. H. Pritchard and E. M. Terentjev, *Macromolecules*, 2016, **49**, 2843–2852.
54 S. Ikuta, K. Takagi, R. B. Wallace and K. Itakura, *Nucleic Acids Res.*, 1987, **15**, 797–811.
55 L. E. Morrison and L. M. Stols, *Biochemistry (Mosc.)*, 1993, **32**, 3095–3104.